applied sciences

MDPI

Article

The Influence of Ionizing Radiation on Paclitaxel-Loaded Nanoparticles Based on PLGA

Izabela M. Domańska [1], Ramona Figat [2], Aldona Zalewska [3], Krystyna Cieśla [4], Sebastian Kowalczyk [3], Karolina Kędra [5] and Marcin Sobczak [1,*]

[1] Department of Pharmaceutical Chemistry and Biomaterials, Faculty of Pharmacy, Medical University of Warsaw, 1 Banacha Str., 02-097 Warsaw, Poland; izabela.domanska@wum.edu.pl
[2] Department of Toxicology and Bromatology, Faculty of Pharmacy, Medical University of Warsaw, 1 Banacha Str., 02-097 Warsaw, Poland; ramona.figat@wum.edu.pl
[3] Faculty of Chemistry, Warsaw University of Technology, 3 Noakowskiego Str., 00-664 Warsaw, Poland; aldona.zalewska@pw.edu.pl (A.Z.); sebastian.kowalczyk@pw.edu.pl (S.K.)
[4] Institute of Nuclear Chemistry and Technology, 16 Dorodna Str., 03-195 Warsaw, Poland; k.ciesla@ichtj.waw.pl
[5] Institute of Physical Chemistry, Polish Academy of Sciences, 44/52 Kasprzaka St., 01-224 Warsaw, Poland; kkedra@ichf.edu.pl
* Correspondence: marcin.sobczak@wum.edu.pl; Tel.: +48-22-572-0783

Abstract: The effect of ionizing radiation (γ-rays and electron beam) on anticancer drug delivery systems (DDSs) properties was evaluated concerning potential sterilization. For this purpose, paclitaxel (PTX)-loaded nanoparticles were obtained using a biodegradable, self-developed copolymer of L-lactide and glycolide (PLGA), synthesized in the presence of bismuth 2-ethylhexanoate catalyst. The nanoparticles were obtained with a high encapsulation efficiency of PTX (*EE* = 94.2%). The average size of the nanoparticles was 253.5 nm. The influence of irradiation (sterilization dose, 25 kGy) on the microstructure and the physicochemical and thermal properties of the polymer matrix was investigated, as well as the effect of irradiation on the morphology and physicochemical properties of the pharmaceutical formulations of the nanoparticles. Additionally, an in vitro drug release study was conducted regarding any alterations in the kinetic profiles of drug release. It was confirmed that the irradiation with both types of ionizing radiation, i.e., γ-rays and electron-beam (EB), slightly decreased the average molecular weight of the polymer matrix. While only negligible changes in the microstructure and thermal properties of PLGA were observed after irradiation with EB, the average length of lactidyl blocks (l_{LL}) in the copolymer chains irradiated with γ-rays decreased from 4.33 to 3.35. Moreover, the contribution of crystalline phase (X_c) in γ-irradiated samples decreased significantly from 35.1% to 22.7%, suggesting a dominant mechanism of chain scission over cross-linking in PLGA samples irradiated with γ-rays. In vitro drug release results demonstrate a sustained and controlled release of PTX from the nanoparticles based on PLGA. The kinetics of drug release was defined as first order with non-Fickian diffusion. Only negligible differences in the kinetic profiles of PTX release from PLGA drug carriers were observed after irradiation. The overall results suggest good resistance of PLGA nanoparticles to irradiation within the conditions used and the great potential of EB in the sterilization process of the polymeric DDSs.

Keywords: drug delivery systems; radiation sterilization; electron beam; gamma irradiation; paclitaxel; biodegradable polymers; L-lactide and glycolide copolymers; nanoparticles

Citation: Domańska, I.M.; Figat, R.; Zalewska, A.; Cieśla, K.; Kowalczyk, S.; Kędra, K.; Sobczak, M. The Influence of Ionizing Radiation on Paclitaxel-Loaded Nanoparticles Based on PLGA. *Appl. Sci.* **2023**, *13*, 11052. https://doi.org/10.3390/app131911052

Academic Editor: Domenico Lombardo

Received: 5 September 2023
Revised: 30 September 2023
Accepted: 5 October 2023
Published: 7 October 2023

1. Introduction

Cancer is a leading cause of death worldwide. According to the World Health Organization (WHO), the most common cancer types in 2020 were breast and lung cancer. Although breast cancer is characterized by a high cure rate when detected early, lung cancer was the most common cause of cancer deaths in 2020 (1.8 million deaths) [1]. It is,

therefore, of great importance to provide new solutions and new drug forms for anticancer therapy in combination with drug substances already placed on the market. Paclitaxel is a potent anticancer agent of natural origin that was originally isolated from yew bark (*Taxus brevifolia*). PTX is widely used in anticancer therapy, namely, in the treating of breast, ovarian, and non-small cell lung cancers, along with malignant melanoma and leukemias [2,3]. However, its low aqueous solubility is challenging considering the method of administration. For this reason, the entrapment of PTX into nanoparticulate systems has been extensively studied. Polymeric nanospheres reduce the side effects of cytostatics, enhance their tumor deposition and improve therapeutic efficacy. The advantage of DDSs over traditional drug forms results from controlled and sustained drug release in the body [4]. The most desirable drug carriers are obtained from biodegradable and biocompatible polyesters. These polymers, when introduced to the organism, are metabolically decomposed into completely removable and non-toxic products. Nevertheless, polymer drug carriers administered parenterally, are required to withstand the harsh conditions of the sterilization process. Considering biodegradable polyester drug carriers, the assurance of sterility is particularly challenging. Polyesters are thermally unstable; therefore, the number of potentially available sterilization methods is limited, mainly to aseptic filtration. The assurance of sterility under this method is very costly and demanding, and most importantly, for sterile filtration, membranes of a max. 0.22 μm pore size are recommended for use [5]. This, in turn, limits the use of this method in relation to particles size. Moreover, sterile filtration may be questioned from the safety point of view due to feasible microbiological contamination. Therefore, it is of great interest to find an effective, alternative method to enable the maintenance of sterility criteria without altering the physicochemical properties of the sterilized material. Among other commonly used sterilization methods are dry-heat, ionizing radiation, steam, the use of chemicals, and UV. Due to high temperatures applied, dry-heat and steam are excluded for heat- and moisture-sensitive polyester-based materials. High temperatures used in the sterilization process may alter the physicochemical and mechanical properties of polymer matrix and consequently alter the kinetic profile of drug release. Recently, Tapia-Guerrero et al. [6] presented preliminary studies on the use of UV and gamma photons for the sterilization of PLGA nanoparticles. They indicated that the use of UV can be an effective sterilization procedure and, at the same time, not cause significant changes in the physicochemical parameters of nanoparticles. However, the penetration depth of UV rays is very low [7] and therefore is limited mainly to surfaces and transparent scaffolds. The use of chemicals, such as gaseous ethylene oxide, or other highly volatile substances such as formaldehyde, may be applicable for heat- and moisture-sensitive materials. However, some harmful residues may remain within the polymer matrix [8]. Furthermore, using chemicals may alter the polymer's physicochemical properties by reacting with its functional groups [9]. On the other hand, ionizing radiation is the method of choice, gaining an increasing interest of scientists for terminal sterilization of DDSs. The use of the pharmacopeial recommended dose, 25 kGy, is considered adequate for sterilizing purposes [5,10–13]. Irradiation may be conducted under various conditions, including the presence of an inert gas atmosphere, room temperature, or cryogenic conditions. Two types of ionizing radiation are commonly used in the sterilization process, i.e., γ-irradiation and EB. The main advantage of irradiation with γ photons is its high penetration power. Gamma irradiation may be applied for non-uniform and high-density products. Like γ-ray, sterilization with EB is also instantaneous with high-dose delivery. However, it should be considered that sterilization efficiency varies depending on the material used.

Overall, radiation sterilization may be suitable for heat-sensitive drugs or drug carriers. It is a fast and effective process, providing high penetration power through the material. Nevertheless, specific undesirable changes caused by ionizing radiation may occur. Radiation-induced chain scission may lead to polymer fragmentation and consequently a decrease in average molecular mass (M_n) [14]. Moreover, the diminution in M_n is expected to increase with increased irradiation dose. In turn, this may alter the physicochemical

properties of drug carriers [15]. It is, therefore, essential to properly validate the sterilization procedure concerning any potential effects of irradiation, irrespectively, for each type of sterilized product.

In this study, we investigate the influence of γ-rays and EB (25 kGy) on the sterilization process of PTX-loaded polymeric nanoparticles based on self-synthesized polymer matrices. For this purpose, biodegradable copolymers of L-lactide (L-LA) and glycolide (GA) were synthesized in the presence of a bismuth catalyst system, and the effect of irradiation on this polyester DDSs was examined as well.

There is a number of already-published studies on the influence of ionizing radiation on polymeric matrices. However, only a few studies have dealt with the use of γ and EB irradiation for the sterilization purposes of polyester micro-/nanoparticles containing PTX (e.g., Wang et al. [16], who analyzed PTX-loaded PLGA microparticles (LA:GA = 50:50), and Song et al. [17], who analyzed PTX-loaded polylactide microspheres). Our study tries to fill this gap. What is more, these articles are based on the polymers of different monomer composition, therefore cannot be directly compared.

2. Materials and Methods

2.1. Materials

L-Lactide (L-LA, (3S)-*cis*-3,6-Dimethyl-1,4-dioxane-2,5-dione, 98%), poly(vinyl alcohol) (PVA, M_w = 13–23 kDa, 87–89% hydrolyzed), Cremophor® EL and poly(ethylene glycol) (PEG, M_n = 200 Da) were purchased from Sigma-Aldrich Co. (Poznań, Poland). Glycolide (GA, 1,4-Dioxane-2,5-dione, 98%) was purchased from TCI Europe N.V. Co. (Zwijndrecht, Belgium), and bismuth 2-ethylhexanoate ($BiOct_3$) was obtained from Alfa Aesar Co., which is part of Thermo Fisher Scientific (Kandel, Germany). Methanol (CH_3OH, analytical pure), chloroform ($CHCl_3$, analytical pure), dichloromethane (DCM, CH_2Cl_2, analytical pure) and hydrochloric acid (HCl, 35–38%) were obtained from POCH Co. (Gliwice, Poland). Acetonitrile (ACN, gradient grade for liquid chromatography) and trifluoroacetic acid (TFA, ≥99.0%) were purchased from Merck KGaA (Darmstadt, Germany), and phosphate-buffered saline (PBS, pH = 7.4) from Carl Roth GmbH + Co. KG (Karlsruhe, Germany). Paclitaxel (PTX, T45) was received from the Medical University of Gdańsk (Gdańsk, Poland).

2.2. Synthesis of Homo- and Copolymers via *Ring-Opening Polymerization*

The polymeric matrices were synthesized in bulk by the ring-opening polymerization (ROP) of L-LA and glycolide. The monomer composition was 0.85:0.15 (L-LA:GA). The polymerization process was performed under a dry argon atmosphere at 120 °C in the presence of a bio-safe bismuth catalyst system consisting of $BiOct_3$ (catalyst) and PEG200 (co-initiator). The monomer to PEG200 ratio was 100:1. The resulting polymers were purified using the precipitation method (with cold methanol) and dried under a vacuum. The polymers were stored at 4 °C until further usage.

2.3. Preparation of Paclitaxel-Loaded Nanoparticles

The nanoparticles were prepared by a single emulsion (*o*/*w*) solvent evaporation technique. For this purpose, PTX was dissolved in DCM and then poured into a pre-weighed polymer. The drug-to-polymer ratio was 1:10 (*w*/*w*), with a drug concentration of 2 mg mL^{-1}. After complete dissolution, the solution was added dropwise to a 1% PVA aqueous solution to form an o/w emulsion and emulsified (10,000 rpm, T25 digital ULTRA-TURRAX®, IKA, Staufen, Germany). The emulsion obtained was sonicated with 70% amplitude (Vibra Cell 505, SONICS & MATERIALS, INC., Newtown, CT, USA). After the evaporation of the organic solvent, the suspension was centrifuged at 20,000 rpm (Optima XPN-80 Ultracentrifuge, BECKMAN COULTER, Indianapolis, IN, USA) and washed twice to remove the residual emulsifier. The resulting nanoparticles were freeze-dried and stored at 4 °C for further usage.

2.4. Irradiation of Nanoparticles and Polymeric Matrices

The gamma irradiation of the samples was performed using ^{60}Co source in Gamma Chamber 5000 (BRIT, Navi Mumbai, India). The samples were irradiated with a dose of 25 kGy at a dose rate of 1.8 kGy h^{-1} in air and at ambient temperature.

Electron irradiation was performed in a linear electron accelerator Elektronika 10/10 with e-beam energy of 10 MeV using a dose of 25 kGy in air and at ambient temperature.

2.5. Structural Analysis of Polymers

The ^{1}H spectra of the polymers were acquired using an Agilent spectrometer (400 MHz) with 32 scans and a 2.56 s acquisition time. Deuterated chloroform was used as a solvent. The measurements were carried out at room temperature with 32 scans and 2.56 s acquisition time.

The ^{13}C NMR spectra of the samples were recorded at 300 MHz using a Varian spectrometer. Deuterated chloroform was used as a solvent. The measurements were carried out at room temperature with 10,000 scans and 1.73 s acquisition time.

The conversion of the reaction was determined by ^{1}H NMR spectroscopy. Polymer composition, chain microstructure and the yield of transesterification processes were defined by means of ^{13}C NMR spectroscopy measurements [18,19].

2.6. Gel Permeation Chromatography

The M_n value and dispersity index ($Đ$) of each sample were determined by gel permeation chromatography (GPC) using a Viscotek system comprising GPCmax and TDA 305 (triple detection array (TDA): RI, IV, LS) and equipped with DVB Jordi gel column(s) (linear, mixed bed). GPC was performed at 30 °C with DCM as an eluent with a flow rate of 1.0 mL min^{-1}. The calibration was performed using a set of 12 sharp polystyrene standards and a refractometer as a concentration detector.

2.7. Biological Assay

The cytotoxicity of the polymer was evaluated according to the ISO 10993-5:2009 guideline [20], i.e., by the neutral red uptake (NRU) test using BALB/c 3T3 clone A31 mice fibroblasts cell line (American Type Culture Collection). The BALB/3T3 clone A31 line used in the assay is recommended by ISO experts for the NRU cytotoxicity assessment test [20]. The polymeric extracts were prepared by incubating the samples in 1 mg mL^{-1} DMEM medium with 10% bovine serum (24 h, 37 °C) with stirring. The extracts were sterilized using a syringe filter. Highly cytotoxic latex and non-cytotoxic polyethylene were used as reference materials. The samples were considered cytotoxic if they reduced cell survival below 70% when compared to the untreated cells.

The genotoxicity of the polymeric materials was evaluated according to ISO 13829:2000 guideline [21], i.e., by the umu-test using *Salmonella typhimurium* TA3515/psk1002 (Deutsche Sammlung von Mikroorganismen und Zellkulturen GmbH, Germany). The principle of genotoxicity assessment by the umu-test is based on the use of the genetically engineered *Salmonella typhimurium* strain TA3515/psk1002, carrying the umuC-lacZ fusion plasmid. When the SOS response is induced by genotoxins, the umuC-lacZ fusion gene is expressed, and the umuC-lacZ fusion product protein is induced. Since this protein has β-galactosidase activity, it is possible to check the inductivity of umuC gene expression by measuring its activity colorimetrically. The experiment was conducted with and without metabolic activation (S9 rat liver fraction). The polymeric samples were incubated in PBS buffer (GIBCO) for 24 h at 37 °C. The extracts were sterilized by filtration before the assay. The 2-aminoanthracene and 4-nitroquinoline N-oxide were used as positive controls. The genotoxic potential of the samples was determined by Induction Ratio (*IR*). Samples were considered genotoxic when the *IR* value was min. 1.5.

2.8. Thermal Properties

DSC studies were carried out for the polymer matrix that was (a) non-irradiated, (b) γ-irradiated, and (c) irradiated with EB by using a Q200 apparatus (TA Instruments, New Castle, DE, USA). The measurements were performed in a heating/cooling/heating cycle from −50 °C to 180 °C and at a heating/cooling rate of 10 °C min^{-1}. The samples were placed in closed aluminum pans under a constant nitrogen flow. The characteristic temperatures of the occurring crystallization and melting processes were determined as the maximum or minimum of the exothermal (crystallization) and endothermal (melting) processes (T_c, T_m, T_{min}).

The crystalline phase content (X_c) was calculated based on the enthalpy values (Equation (1)) determined from the first heating run:

$$X_c = \frac{\Delta H_m - \Delta H_c}{\sum_i (W_i \times \Delta H_{mi,100\%})} \quad (1)$$

where ΔH_m and ΔH_c are the enthalpies of melting and cold crystallization, respectively; W_i is the weight fraction of the co-monomeric units in the polymer; and $\Delta H_{mi,100\%}$ is the enthalpy of melting for 100% crystalline polymer, which is set at 106 J g^{-1} (polylactide) [22] and 191 J g^{-1} (polyglycolide) [23].

Glass transition was determined based on DSC curves recorded during the second heating run when the polymer was already stabilized, mainly because the glass transition was difficult to isolate from other processes occurring during the first heating.

2.9. Dynamic Light Scattering

The average size and dispersity index (*PDI*) of the prepared nanoparticles were measured by dynamic light scattering (DLS) using a Zetasizer Nano ZS analyzer (Malvern Panalytical Ltd., Malvern, UK). For this purpose, an appropriate amount of the nanoparticles was resuspended in purified deionized water. The zeta-potential (ZP) was determined by electrophoresis in a capillary cell.

2.10. Surface Morphology

The morphology of the nanoparticles was evaluated by scanning electron microscopy (SEM) using an Ultra Plus microscope (ZEISS, Oberkochen, Germany). For this purpose, a small amount of the samples was stuck on a double-sided tape attached to a metal stub and sputter-coated with a thin layer of gold before the measurements.

2.11. Drug Content

To determine the drug content, a certain amount of PTX-loaded nanospheres was dissolved in ACN. The samples were assayed by high-performance liquid chromatography (HPLC) at λ = 229 nm, according to Stefanowicz et al. [3]. The HPLC system was the Beckman Coulter system (Miami, FL, USA). Chromatographic separations were carried out using a Luna C18(2) column (25 cm, 5 µm, 100 A, Phenomenex, Torrance, CA, USA). Chromatographic conditions were a mobile phase consisting of ACN/water/methanol (60/2/38, *v*/*v*/*v*) with TFA (0.1%), and a flow rate of 1 mL min^{-1}. The analyses were performed at 30 °C.

Encapsulation efficiency (*EE*) was calculated according to the following equation (Equation (2)):

$$EE(\%) = \frac{m_e}{m_t} \times 100\% \quad (2)$$

where m_e is the amount of the drug entrapped in the nanoparticles, and m_t is the total amount of drug added.

Drug loading capacity (*DL*) was calculated according to the following formula (Equation (3)):

$$DL(\%) = \frac{m_e}{m_n} \times 100\% \quad (3)$$

where m_e is the amount of the drug entrapped in the nanoparticles, and m_n is the total weight of nanoparticles.

2.12. In Vitro Drug Release Study

In vitro drug release tests were performed using the dialysis method on free PTX as a control and PTX-loaded nanospheres that were (a) non-irradiated, (b) irradiated with γ-rays, and (c) irradiated with EB. PBS solution (pH = 7.4), containing Cremophor® EL (0.5% (*w*/*v*) as a solubilizer, was used as a release medium. The suspensions were maintained at 37 °C while stirring at 100 rpm (ES-20, Biosan, Riga, Latvia). The amounts of PTX released from the samples were chromatographically determined at λ = 229 nm, according to Section 2.11.

The results of the PTX release were analyzed according to zero-order, first-order, Higuchi and Korsmeyer–Peppas mathematical models, as shown in Equations (4)–(7) [24,25].

Zero order:

$$F = kt \quad (4)$$

First order:

$$logF = logF_0 - \frac{kt}{2.303} \quad (5)$$

Higuchi model:

$$F = k\sqrt{t} \quad (6)$$

Korsmeyer–Peppas model:

$$F = kt^n, for\ F < 0.6 \quad (7)$$

where F is the fraction of drug released in time (t), F_0 is the initial concentration of the drug, k is the model constant, and n is the release exponent.

3. Results and Discussion

The aim of this research was to develop nontoxic PLGA systems for the controlled release of PTX. The DDSs obtained in this work are intended for biomedical application and therefore require sterilization. For this purpose, the use of ionizing radiation (γ-rays and EB, 25 kGy) as a potential sterilization technique was proposed. The influence of irradiation on the structure and physicochemical properties of polymeric nanoparticles, as well as the kinetic profile of PTX release, was analyzed in detail.

3.1. Synthesis and Characterization of Polymers

The copolymer of L-lactide and glycolide with monomer composition L-LA:GA = 0.85:0.15 was synthesized using a bismuth catalyst system, consisting of the catalyst, Bi-Oct_3, and the co-initiator, PEG200, leading to the formation of a linear polyester.

Importantly, the polymeric matrix obtained was neither cyto- nor genotoxic, which is critical in biomedical applications. In order to assess the cytotoxicity of the polymer, the NRU test was performed. It was observed that for the highest concentrations of the extracts tested (1 mg mL^{-1}), the cell survival rate was 106 ± 6% when compared to untreated cells (Table 1). These results confirmed the lack of cytotoxic effect of the PLGA sample tested. The umu-test with and without metabolic activation was used to assess the

genotoxicity of the polymer. At the highest concentration tested (1 mg mL^{-1}), the PLGA samples did not inhibit the growth of Salmonella typhimurium cells (G > 0.5). This, together with the induction ratio (IR) being lower than 1.5, indicates the lack of genotoxicity of the polymer (Table 1).

Table 1. Results of umu- and NRU tests (concentration 1 mg mL^{-1}).

Sample	Genotoxicity Assay				Cytotoxicity Assay
	−S9 [a]		+S9 [b]		
	G	IR [a]	G	IR [b]	Cells Viability (%)
PLGA	0.97 ± 0.07	0.80 ± 0.07	0.97 ± 0.07	1.31 ± 0.40	106 ± 6
Positive Control	1.04 ± 0.01	3.30 ± 0.28	0.87 ± 0.04	2.53 ± 0.41	1 ± 1
Negative Control	1.00 ± 0.01	1.00 ± 0.05	1.00 ± 0.04	1.00 ± 0.08	111 ± 1

[a] version without metabolic activation; [b] version with metabolic activation.

The results of the copolymerization of L-lactide with glycolide are presented in Table 2. The polymerization reached 94.5% conversion of L-LA and the near-complete conversion of GA. The synthesized polymer was irradiated using γ-rays and EB with a dose of 25 kGy. Molecular masses and dispersity coefficients of irradiated and non-irradiated PLGA samples were determined by GPC in triplicate. The resulting polymer was characterized by a low dispersity index ($Đ$ = 1.83), and the average molecular mass M_n = 13.8 kDa (Table 2), which was in line with the calculations based on the monomer feed ratio (M_n ~14.5 kDa). As it is shown in Table 2, a considerable decrease in M_n was observed for the copolymer subjected to both γ-rays and EB (13.8% and 14.1% of M_n decrease for PLGA samples irradiated with γ-rays and EB, respectively) along with an increase in dispersity. Interestingly, no significant difference between the influence of γ-rays and EB on the M_n of PLGA was observed. In comparison, in our previous research [26] describing the influence of irradiation on PTX-loaded nanoparticles of different polymer matrices (poly(L-lactide)—PLA, poly(ε-caprolactone)—PCL, the copolymer of L-LA and ε-caprolactone—PLACL, and the copolymer of GA and ε-caprolactone—PCLGA), a relatively higher decrease in M_n was observed for γ-irradiated copolymers (ΔM_{nPLACL} = −12.7%, ΔM_{nPCLGA} = −28.2%) compared to the copolymers irradiated with EB (ΔM_{nPLACL} = +5.5%, ΔM_{nPCLGA} = +3.2%) [26]. The overall decrease in the molecular mass of PLGA observed after the irradiation process may suggest that the chain scission was a leading mechanism, taking place during the sterilization of the polymer by both γ-rays and EB. This is consistent with the literature, according to which the dominant mechanism for PLGA irradiated with low doses of γ-rays and EB is chain scission [27,28]. During the irradiation, PLGA is excited, and active species, such as free radicals, are formed. The active species initiate further reactions, causing bond cleavage among the polymer chain. As a result, the molecular mass of the polymer is lowered [28].

Table 2. The influence of irradiation on the microstructure and physicochemical properties of PLGA.

Irradiation	M_n (kDa) [a]	ΔM_n (%) [ab]	$Đ$ [a]	F_{GG}	l_{LL}^e	l_{GG}^e	$T_{II\ (LGL)}$	$T_{II\ (GLG)}$
non-irr	13.79 ± 0.10	n.a.	1.83 ± 0.01	0.15	4.33	1.23	0.15	1.14
irr-γ	11.89 ± 0.64	−13.82	1.95 ± 0.09	0.16	3.35	1.28	0.13	1.38
irr-e$^-$	11.85 ± 0.15	−14.07	1.96 ± 0.03	0.16	4.61	1.22	0.15	0.79

n.a.—not applicable; [a]—determined by GPC; [b]—M_n change compared to non-irradiated sample; F_{GG}—mole fraction of glycolidyl units in the copolymer chain; l_{LL}^e—experimental average length of

lactidyl blocks; l_{GG}^{e}—experimental average length of glycolidyl blocks; T_{II}—yield of the second mode of transesterification.

The microstructure of the polymers was investigated using ^{13}C NMR spectroscopy. The characteristic signals were assigned to corresponding co-monomeric sequences by analogy according to the literature [19]. As seen in Figure 1, the signal for consecutive –LLL– sequence (169.65 ppm, Table 3) dominated over other signals due to the high LA-to-GA ratio in the feed (LA:GA = 85:15). However, the presence of odd sequences, such as –LGL– and –GLG–, was also noticed, indicating the participation of the transesterification of the second mode accompanying the polymerization process. As a result, the obtained polymer was of a random structure and short average lengths of blocks (Table 2).

Table 3. Chemical shift in ^{13}C NMR spectrum of PLGA.

Chemical Shift (ppm)	Sequence
169.65	LLLL
169.58	LLGG
169.50	LGLL
169.47	GGLL
169.38	GLG
166.55	GGLG
166.49	GGLL
166.47	GGGG
166.44	LGL
166.38	LLGG

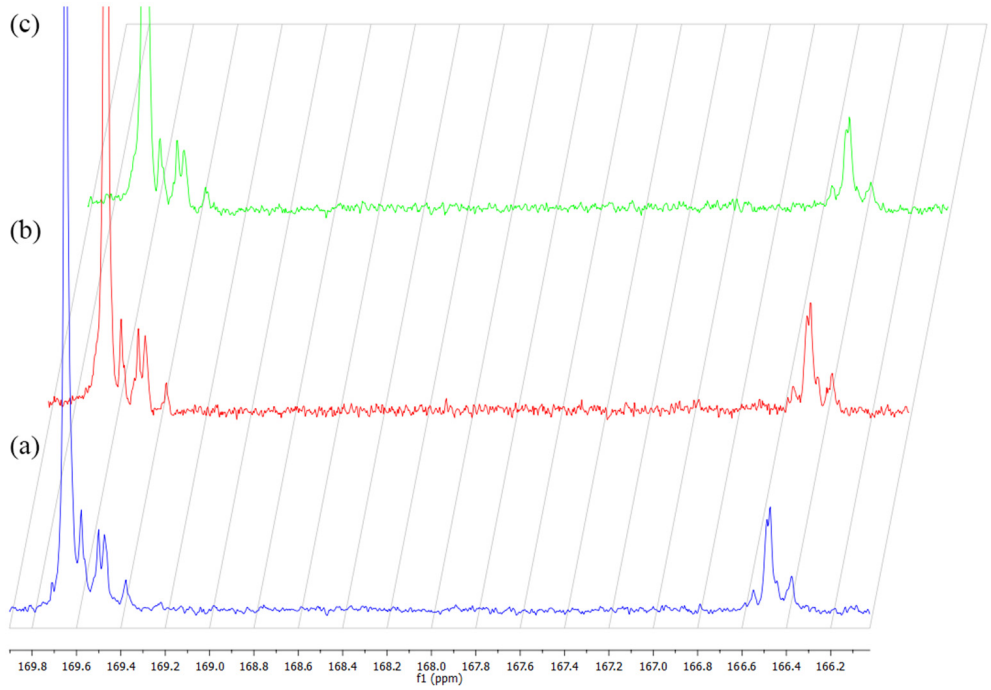

Figure 1. The influence of ionizing radiation on ^{13}C NMR spectra of PLGA non-irr (**a**), irr-γ (**b**) and irr-e^{-} (**c**).

As seen in Figure 1, no additional signals were found in the ^{13}C NMR spectra upon irradiation. Additionally, a detailed analysis of the polymer microstructure revealed only negligible changes in relation to the average length of glycolidyl units (l_{GG}^{e}) and $T_{II[LGL]}$ (Table 2). As seen from the value of T_{II} of lactyl units (L) ($T_{II[GLG]}$ = 1.11), the synthesized polymer was of a random structure. After irradiation with γ-rays, $T_{II[GLG]^{\gamma}}$ increased to

1.38, and the average length of lactidyl units (l_{LL}) decreased from 4.33 to 3.35. These slight differences may suggest that the irradiation might cause some changes in the regions of the lactidyl units of the copolymer chain. It appears that the relative amount of –GLG– sequences in the copolymer increased after irradiation with γ-rays, possibly as a result of chain scission. However, after the irradiation of PLGA with EB, $T_{II[GLG]}$ slightly decreased ($T_{II[GLG]}^{EB}$ = 0.79), and l_{LL} increased from 4.33 to 4.61. It has to be taken into consideration that irradiation with EB was conducted with a high dose rate in considerably lower time compared to irradiation in a gamma chamber. In fact, exposition in a gamma chamber needs a dozen hours to obtain a dose of 25 kGy, and there is enough time that free radicals reactions leading to chain scission may occur with high efficiency, especially in the presence of atmospheric oxygen. On the contrary, during exposition in EB, a considerable amount of radicals are formed in a short time. These (high molecular) radicals might recombine; thus, the processes of cross-linking become more probable. Additionally, due to limited contact with oxygen, degradation processes may also be limited, compared to irradiation with γ rays. As a result, these processes may lead to chain elongation.

The overall results, i.e., decrease in molecular mass and changes in the polymer microstructure after irradiation, may be explained in terms of two concurring processes taking place during irradiation (chain scission and cross-linking). However, the overall decrease in the M_n of PLGA suggests the predominance of chain scission over cross-linking. According to the literature, lactidyl units may be more susceptible to irradiation than glycolyl units (G) due to the presence of tertiary carbon atoms, which, together with ester linkages, are the important sites for bond cleavage [9,27]. Therefore, the changes in the microstructure were more apparent in the values of T_{II} and average block lengths related to lactidyl units.

3.2. The Influence of Ionizing Radiation on Thermal Properties of Polyesters

The influence of ionizing radiation on the thermal properties of PLGA was assessed by DSC. During the first heating of the non-irradiated sample (Figure 2a), a decrease in heat flow was observed at temperatures above 30 °C, possibly connected to the glass transition. It was accompanied by an endothermal effect with the minimum of 77.3 °C. In the higher temperature range, the exothermal effect of cold crystallization (recrystallization of the polymer chains into the structure with lower energy; T_c = 103.7 °C) was observed. It was followed by the endothermal effect with two minima (at 138.0 °C and 147.1 °C). The two minima of the endothermal effect can be related to a superposition of the melting of different supramolecular structures of the polymer and, precisely, to the melting of less- and better-ordered crystals [29]. Loo et al. [30] attributed them to the melting of the more tightly packed linear polymer fraction (at higher temperature) and the more branched chains (at lower temperature).

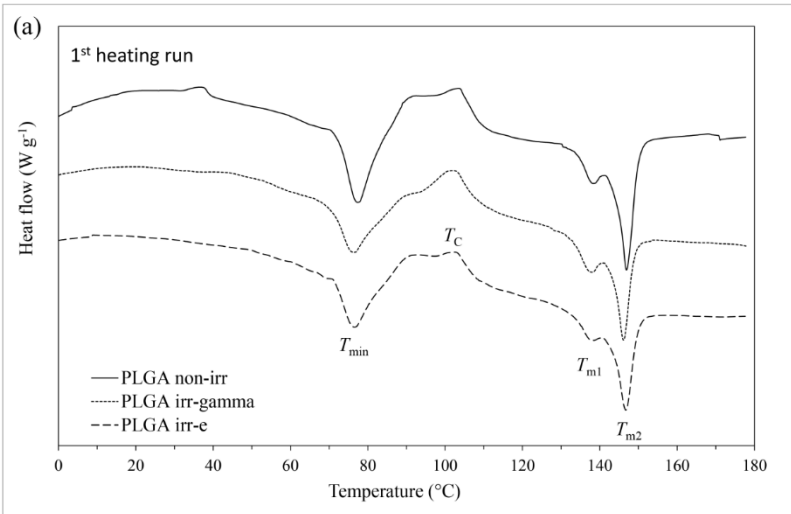

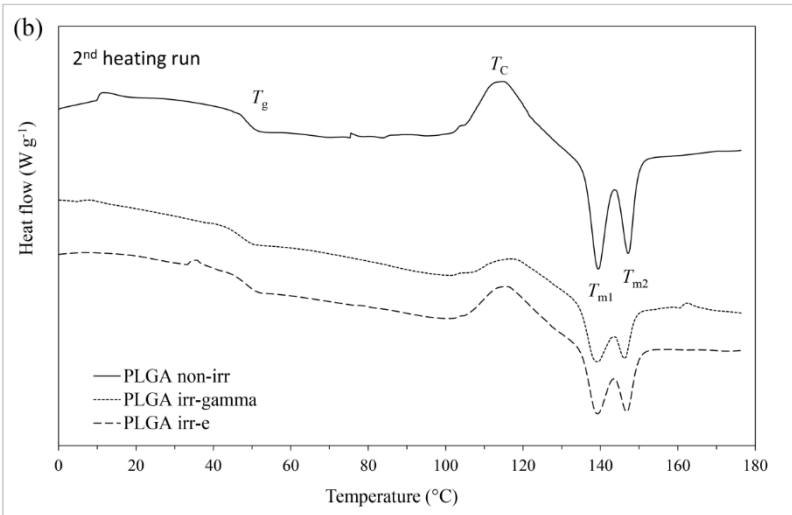

Figure 2. DSC curves of non-irradiated PLGA and PLGA irradiated with γ-rays and EB: (**a**) 1st heating run and (**b**) 2nd heating run.

The genesis of the endotherm accompanying the glass transition (T_{min} = 77.3 °C) is not entirely clear. It can be considered as related to the melting of the low-ordered fractions of PLGA, that are possibly characterized by the polymer of low molecular weight (oligomers). It follows the hypothesis given by Dorati et al. [31], who related the endothermal peak between 20 °C and 40 °C of PEG-PLGA samples to the melting of free PEG-PLGA blocks of the polymer that were formed during storage or as a result of radiation-induced degradation [31].

During the second heating (Figure 2b), the initial sample undergoes recrystallization followed by melting, with the enthalpies of both processes being similar (48–50 J g^{-1}) (indicating that almost all of the melted material was formed during recrystallization occurring at a lower temperature during the same heating cycle). Moreover, these enthalpies were similar to the enthalpy of melting occurring on first heating.

Based on the above data, the copolymer was found to reveal a semicrystalline structure (X_c = 35.1%). Additionally, single T_g indicates good homogeneity of the copolymer. The influence of ionizing radiation on the thermal and crystalline properties of PLGA is shown in Table 4. No change in T_g was observed after irradiation with EB, whereas a relatively small effect was observed after the gamma irradiation (decrease from 48.1 °C to 47.6 °C). However, the changes were noticed in the enthalpies and characteristic temperatures of the crystallization and melting processes (Table 4). This was particularly evident in the enthalpies of the processes. It was also noticed that the effect of gamma irradiation was higher than that of EB.

Table 4. The influence of ionizing radiation on thermal parameters of PLGA determined from DSC.

Irradiation	T_g [b] (°C)	T_{min} [a] (°C)	T_c [a] (°C)	T_m [a] (°C)	ΔH_c [a] (J g^{-1})	ΔH_m [a] (J g^{-1})	X_c [a] (%)
non-irr	48.1	77.3	103.7	138.0 (T_{m1}) 147.1 (T_{m2})	8.52	50.16	35.1
irr-γ	47.6	76.8	102.6	137.4 (T_{m1}) 146.2 (T_{m2})	15.00	41.92	22.7
irr-e-	48.2	76.7	103.3	137.3 (T_{m1}) 146.5 (T_{m2})	4.76	42.06	31.4

[a] determined from the 1st heating run; [b] determined from the 2nd heating run.

It can be concluded that ionizing radiation induces a decrease in the crystalline phase content. However, the effect was much higher after irradiation in the gamma chamber

compared to irradiation with EB (X_c decreased from 35.1% to 22.7% and to 31.4%, respectively).

These results, in combination with GPC data (Table 2), may differentiate both types of irradiation (γ-rays and EB) in regard to the type of mechanism prevailing during the irradiation process (crosslinking and/or chain scission). Importantly, the irradiation of the samples was conducted in air. The presence of atmospheric oxygen enables reactions of alkyl radicals with oxygen. In the case of prolonged exposure to radiation in the gamma chamber, this resulted in high participation in the degradation process. However, rapid irradiation with a high dose (as for EB in our case) acts similarly to the exposure of the material to irradiation in an inert gas atmosphere, which prevents the formation of peroxyl radicals within the interior of the material. This occurs because atmospheric oxygen does not have time to diffuse into the sample and cannot react with its interior. In that case, the outer layer of the material (exposed to oxygen), favors oxidative degradation, while some crosslinking may occur inside the material [32]. This may therefore explain the overall decrease in M_n in the case of both types of irradiation, together with the contradictory results of the microstructure of the polymer, which suggests the slight elongation of lactidyl segments (from 4.33 to 4.61) in the copolymer chain irradiated with EB.

Contrary to the non-irradiated copolymer ($\Delta H_c 2nd^{heating}$ = 48.13 J g^{-1} and $\Delta H_m 2nd^{heating}$ = 49.84 J g^{-1}), in the case of both irradiated samples, recrystallization occurred to a much lesser extent during the second heating (as shown by the lower values of ΔH_c being equal to 22.86 J g^{-1} and 29.17 J g^{-1} in the case of the γ-irradiated and EB-irradiated samples, respectively). However, even though the melting enthalpies were lower (31.90 J g^{-1} and 39.68 J g^{-1} in the case of γ-irradiated and EB-irradiated PLGA samples), this indicated a lower crystalline content. Some of the melting crystalline phase was present in the irradiated samples before the start of this heating cycle (as shown by the lower values of ΔH_c compared to ΔH_m), indicating that it was formed during the preceding cooling cycle (desmeared curves). Simultaneously, the appropriate values of T_c were equal to 115.0 °C, 117.8 °C and 116.2 °C, and the values of T_m were equal to 139.4 and 147.2 °C (PLGA non-irr), 139.0 and 146.1 °C (γ-irr PLGA), and 139.1 and 146.6 °C (EB-irr PLGA).

Therefore, it can be concluded that irradiation also influences the recrystallization and melting processes taking place during cooling and the second heating. Similarly to other cases, the effect was more evident after radiation treatment performed in the gamma chamber compared to EB.

3.3. Evaluation of the Stability of PTX-Loaded Nanoparticles to Irradiation

The PTX-loaded nanoparticles were obtained using single solvent evaporation technique with an encapsulation efficiency of PTX of 94.2 ± 3.0%. The *DL* value of PTX was 8.0 ± 0.2%.

Importantly, the HPLC spectra of the PTX extracted from the irradiated nanoparticles (Figure 3) did not show any additional peaks (compared to non-irradiated samples). Moreover, the areas of the peak of PTX (RT ~6 min) obtained from the chromatograms of the non-irradiated and irradiated samples, and recalculated with a given concentration gave an RSD value of 0.4%. This results confirm that PTX did not degrade after irradiation with both types of ionizing radiation (γ-rays and EB) and suggest the stability of PTX encapsulated in polymeric nanoparticles to irradiation (25 kGy).

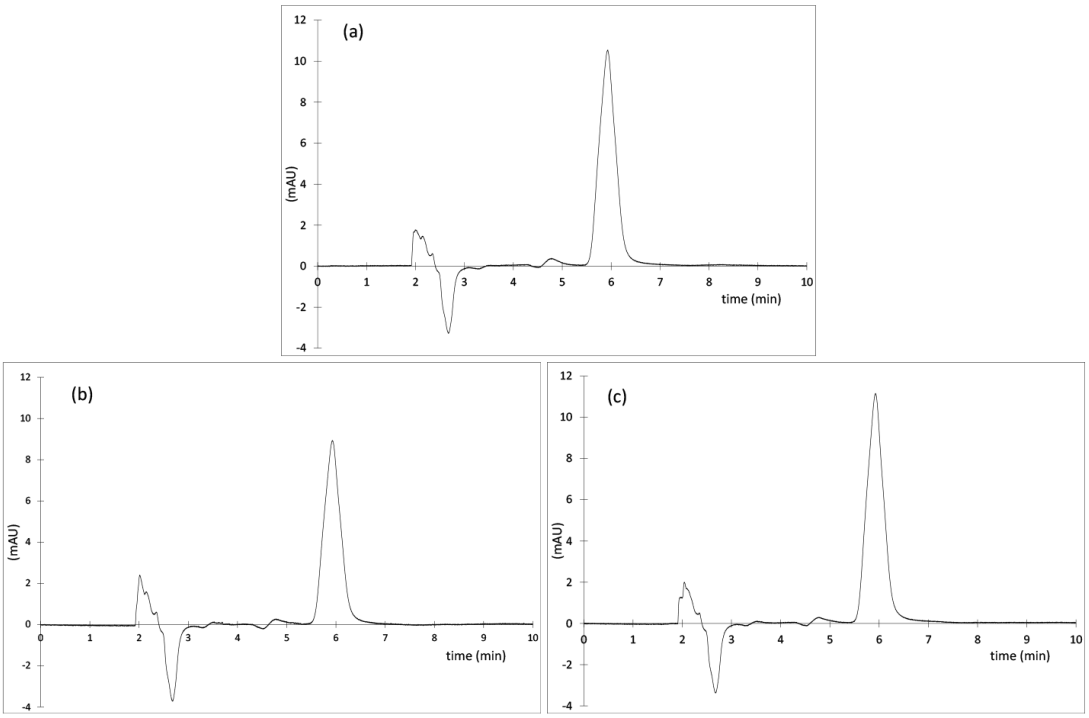

Figure 3. HPLC chromatograms of PTX extracted from the nanoparticles (**a**) non-irradiated (C_{PTX} = 7.6 μg mL^{-1}), (**b**) γ-irradiated (C_{PTX} = 5.6 μg mL^{-1}) and (**c**) irradiated with EB (C_{PTX} = 7.8 μg mL^{-1}).

The resulting particles (independent of drug loading) were spherical in shape (as shown by SEM, Figure 4) and varied in dimensions. No particular differences between the particles morphology were noticed after irradiation. DLS data have shown that the average size of particles was equal to 253.5 ± 3.9 nm with narrow particle size distribution (*PDI* < 0.2) independent of whether the particles were loaded or not (Table 5). No change in average particles size was noticed after the irradiation with γ-rays and EB (compared to non-irradiated samples). The zeta potential of PTX-loaded particles was negative (−20.83 mV) and similar to the formulations prepared without the drug. This might be explained by the lack of ionizable functional groups in PTX molecules [33]. However, after irradiation, *ZP* decreased and reached −36.73 mV and −33.75 mV in the case of γ- and EB-irradiated samples, respectively. This may be attributed to a greater amount of ionized terminal carboxylic groups [34,35] resulting from polymer degradation, which may potentially contribute to the increase in particles stability in suspension.

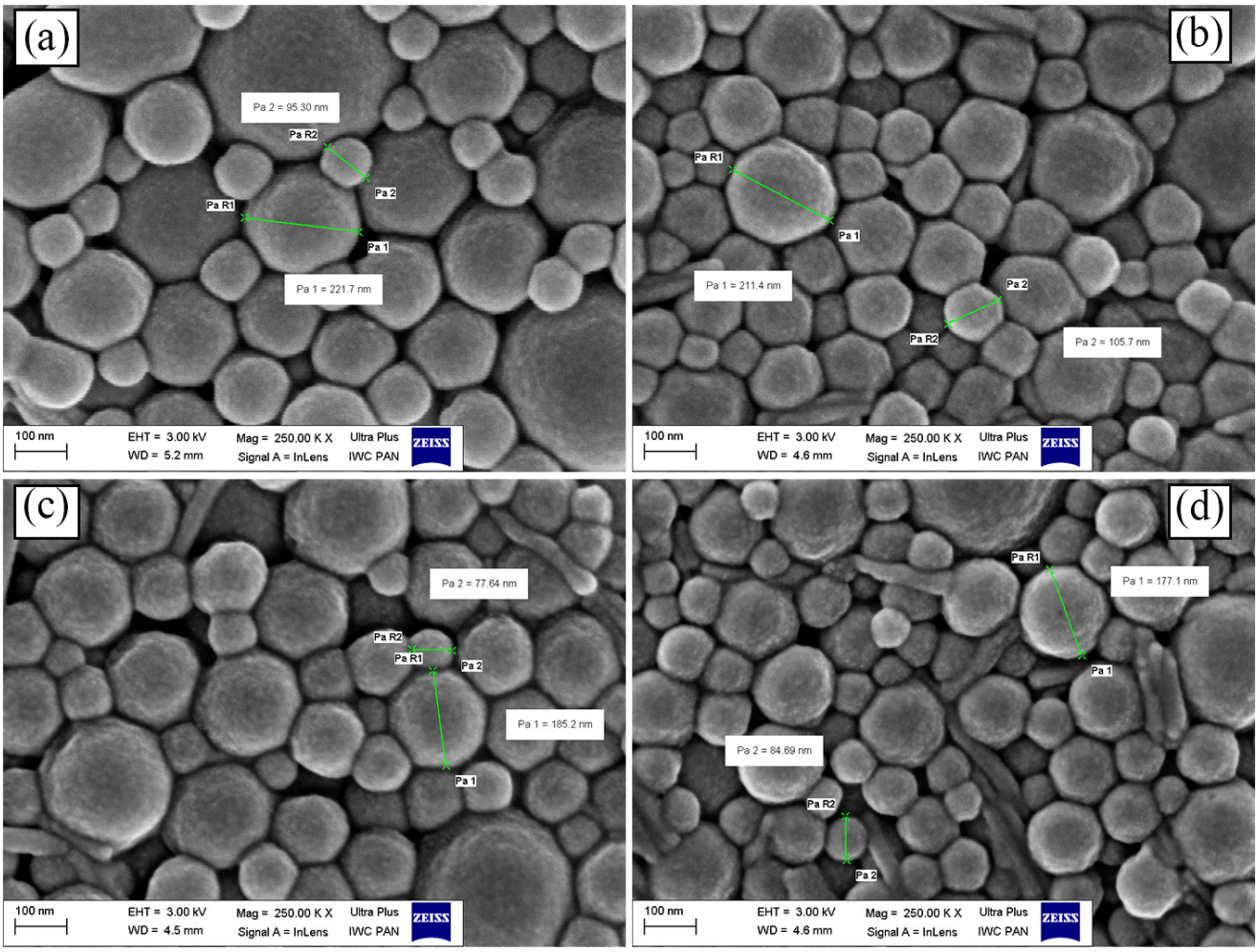

Figure 4. SEM micrographs of lyophilized PLGA nanoparticles: (**a**) placebo, (**b**) non-irr, (**c**) irr-γ and (**d**) irr-e PLGA nanospheres with PTX.

Table 5. The influence of ionizing radiation on PTX-loaded nanoparticles determined by DLS.

Irradiation	Size (nm)	*PDI*	*ZP* (mV)
PLGA	253.6 ± 4.1	0.19 ± 0.03	−22.48 ± 0.41
PLGA-PTX non-irr	253.5 ± 3.9	0.17 ± 0.03	−20.83 ± 1.17
PLGA-PTX irr-γ	256.4 ± 3.1	0.20 ± 0.02	−36.73 ± 1.26
PLGA-PTX irr-e$^-$	253.6 ± 2.1	0.17 ± 0.02	−33.75 ± 0.57

3.4. In Vitro Drug Release

Figure 5 displays cumulative drug release profiles of irradiated and non-irradiated nanoparticle formulations. The release profile of free PTX was added as a control. The release of PTX from PLGA nanoparticles exhibited a monophasic release pattern (no initial burst release was observed). An almost complete drug release was observed after 36 days of the study, independent of applied irradiation. Importantly, the release of free drug was faster compared to the drug release from the nanoparticles. This indicates that the release profiles of the encapsulated drug were not hindered by the dialysis membrane.

The in vitro release mechanism of paclitaxel from the nanoparticles was further evaluated using zero-order, first-order, Higuchi and Korsmeyer–Peppas mathematical release kinetic models (Table 6).

Table 6. Data analysis of PTX release from PLGA nanoparticles.

Irradiation	Zero-Order	First-Order	Higuchi		Korsmeyer–Peppas	
	R^2	R^2	R^2	K_H [a]	R^2	n [b]
non-irr	0.881	0.998	0.981	17.805	0.995	0.793
irr-γ	0.949	0.963	0.991	17.906	0.977	0.857
irr-e	0.946	0.974	0.995	17.820	0.993	0.857

[a]—release rate constant; [b]—release exponent.

The values of R^2 for zero-order and first-order kinetics suggest that the drug release profiles from the PLGA nanoparticles followed the first-order kinetic, regardless of irradiation. Some references, as, e.g., the work of Jusu et.al. [36], demonstrate the zero-order release of paclitaxel from PLGA nanoparticles, and being well characterized by Korsmeyer-Peppas model. However, mathematical models are only a simplification and do not give exact insight into the mechanism of drug release. Moreover, the composition of the comonomers obtained by us is different from those tested by other authors. It should also be noted that the obtained R^2 values for the zero-order and first-order kinetics models are not very different. Probably, in the case of the obtained nanoparticles, we are dealing with a mixed drug release mechanism.

Additionally, the release data fitted well to the Higuchi and Korsmeyer–Peppas mathematical models. A detailed analysis of the release exponent n from the Korsmeyer–Peppas model ($n_{\text{non-irr}} = 0.79$ and $n_{\text{irr-}\gamma,\text{EB}} = 0.86$) indicates drug release with non-Fickian diffusion ($0.45 < n < 0.89$), in which two mechanisms (diffusion and erosion) take part in drug release [37].

Only negligible differences (in the frame of the scatter of experimental data) in the kinetic profiles of PTX release from PLGA drug carriers were observed after irradiation. This suggests the good resistance of PLGA nanoparticles to irradiation. Despite some degradation observed within the polymer matrix itself, drug release profile from the irradiated samples did not vary significantly compared to the non-irradiated samples. This may be explained to some extent by the radio-protective effect of PTX resulting from its molecular structure. Aromatic groups present in PTX structure act as energy sinks via the energy transfer mechanism and stabilize the molecule [38,39].

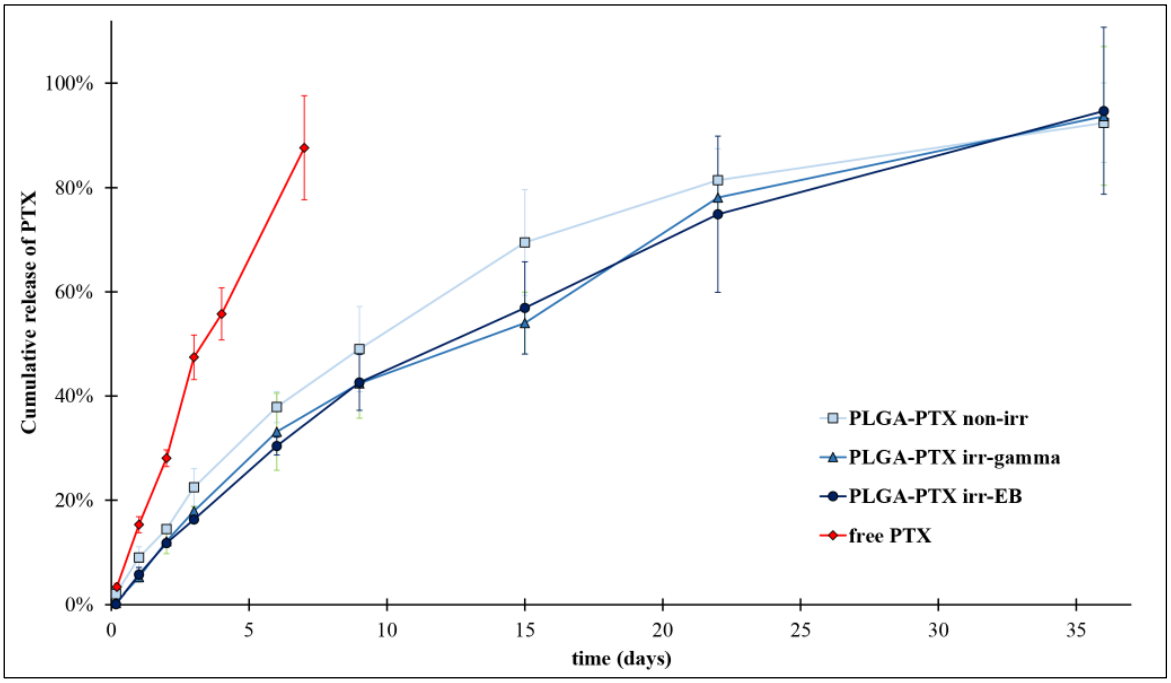

Figure 5. The influence of irradiation on kinetic profiles of PTX release from PLGA nanoparticles.

4. Conclusions

In this study, we demonstrate the feasibility of the radiation sterilization of PLGA nanoparticles containing PTX. Importantly, the polymer matrix synthesized in this study and used as the drug carrier was neither cyto- nor genotoxic, which is required in the case of biomedical applications. The influence of irradiation was analyzed to develop nanoparticles and the polymer matrix itself, and the type of ionizing radiation (γ-rays or EB). Considering the polymer matrix, PLGA exhibited a noticeable degradation degree, given as a decrease in M_n, reaching approx. 14% after irradiation with γ-rays and EB. This result suggests that the main mechanism taking part during the irradiation of PLGA was chain scission. However, the structural changes differed depending on the type of ionizing radiation applied. Gamma-irradiation significantly affected the micro- and macroscopic properties of PLGA by shortening lactidyl segments in the polymer chains. While only negligible changes in characteristic temperatures of the polymer (T_g, T_c, T_m) were observed, the crystallite content decreased from 35.1% to 22.7%. Contrary to irradiation with γ-rays, in the case of the polymer irradiated with EB, a slight elongation of lactidyl blocks was observed. This may be explained by differences in the course of radiation processes. Considering the polymer irradiated with γ-rays, the changes of properties may be assigned with the predominance of chain scission (probably accompanied to some extent by cross-linking), while during irradiation with EB, two processes, that differ in the mechanism of action (chain scission and cross-linking) were likely to occur to a similar extent. While prolonged exposure of the polymer to γ-rays leads to the breakage of polymer chains and the oxidative degradation of the material. In the case of EB, the rapid irradiation of the polymer with a high dose (compared to γ-rays) disables oxygen diffusion into the internal layers of the material. It creates similar conditions as the inert gas atmosphere. As a result, external layers of the polymer undergo oxidative degradation, while cross-linking occurs inside the polymer matrix [32]. This may, therefore, explain the overall decrease in M_n in the case of both types of irradiation and the elongation of lactidyl blocks of PLGA irradiated with EB.

Comparing the effects of the sterilization process with γ-rays and EB on the physicochemical, structural, and thermal properties of PLGA clearly indicates that within this study, EB induced less structural damage to the copolymer.

The nanoparticles were obtained with a high efficiency of PTX encapsulation (*EE* = 94.2 ± 3.0%). The particles characterize a spherical shape and an average size of 253.5 ± 3.9 nm (shown by DLS). The physicochemical analysis of the particles did not reveal any changes in their size and morphology after the sterilization process. A complete release of PTX was achieved within the first 36 days of the study. The nanoparticles released the drug with a first-order kinetic profile and with non-Fickian diffusion (anomalous mechanism). Importantly, the sterilization process (independent of the type of ionization) did not significantly affect the drug's release.

The overall results have shown that PLGA nanoparticles have potential for the sustained delivery of PTX and have proved the great potential of EB for the purposes of sterilization of PLGA-based nanoparticles containing PTX.

Author Contributions: I.M.D.: conceptualization, chemical, structural, analytical and pharmaceutical research, methodology, investigation, formal analysis and writing—original draft; R.F.: biological research, methodology and investigation; A.Z.: DSC measurement and analysis; K.C.: interpretation of thermal analysis data, investigation, formal analysis, writing—original draft, and editing and supervision; S.K.: GPC measurement; M.S.: conceptualization, chemical, structural, analytical and pharmaceutical research, investigation, writing—original draft, editing and supervision. K.K.: interpretation of thermal analysis data, DLS and Zeta potential analysis data, and text correction. All authors have read and agreed to the published version of the manuscript.

Funding: The work was performed as part of Project number FW231/1/F/MBS/N/21, which was carried out from 2021 to 2023 and was funded by the scientific financial support obtained from the Medical University of Warsaw (Poland).

Institutional Review Board Statement: Not applicable.

Informed Consent Statement: Not applicable.

Data Availability Statement: The data presented in this study are available upon request from the corresponding author.

Acknowledgments: The contribution of Izabela M. Domańska was realized within Project No POWR.03.02.00-00-I009/17-00 (Operational Project Knowledge Education Development 2014–2020 co-financed by the European Social Fund).

Conflicts of Interest: The authors declare that they have no known competing financial interest or personal relationships that could appear to have influenced the work described in this paper.

Sample Availability: Samples of all compounds are available from the authors.

Abbreviations

ACN	acetonitrile
$BiOct_3$	bismuth 2-ethylhexanoate
Đ	dispersity index (GPC)
DDSs	drug delivery systems
EB	electron-beam
EE	encapsulation efficiency
GA	glycolide
G	glycolyl unit
GG	glycolidyl unit
ΔH_c	enthalpy of cold crystallization
ΔH_m	enthalpy of melting
IR	induction ratio
L	lactyl unit
LL	lactidyl unit
L-LA	L-lactide
l_{GG}	average length of glycolidyl units
l_{LL}	average length of lactidyl blocks
M_n	number average molecular mass

NRU	neutral red uptake
PBS	phosphate-buffered saline
PDI	dispersity index (DLS)
PEG	poly(ethylene glycol)
PLGA	copolymer of L-lactide and glycolide
PTX	paclitaxel
PVA	poly(vinyl alcohol)
ROP	ring-opening polymerization
T_c	temperature of cold crystallization
TFA	trifluoroacetic acid
T_g	glass transition temperature
T_{II}	transesterification of the second mode
T_m	temperature of melting
X_c	crystalline phase content
ZP	zeta potential

References

1. WHO. Cancer Fact Sheet. 2022. Available online: https://www.who.int/news-room/fact-sheets/detail/cancer (accessed on 26 May 2022).
2. Surapaneni, M.S.; Das, S.K.; Das, N.G. Designing Paclitaxel Drug Delivery Systems Aimed at Improved Patient Outcomes: Current Status and Challenges. *ISRN Pharmacol.* **2012**, *2012*, 623139. https://doi.org/10.5402/2012/623139.
3. Stefanowicz, Z.; Sobczak, M.; Piętniewicz, A.; Kołodziejski, W. Macromolecular conjugates of paclitaxel: Synthesis, characterization, and In Vitro paclitaxel release studies based on HPLC validated method. *Acta Chromatogr.* **2016**, *28*, 99–117. https://doi.org/10.1556/AChrom.28.2016.1.8.
4. Martins, K.F.; Messias, A.D.; Leite, F.L.; Duek, E.A.R. Preparation and characterization of paclitaxel-loaded PLDLA microspheres. *Mat. Res.* **2014**, *17*, 650–656. https://doi.org/10.1590/S1516-14392014005000028.
5. Council of Europe. *Suppl. 9.2. European Directorate for the Quality of Medicines & HealthCare*; Council of Europe: London, UK, 2017, pp. 4333–4350.
6. Tapia-Guerrero, Y.S.; Del Prado-Audelo, M.L.; Borbolla-Jiménez, F.V.; Gomez, D.M.G.; García-Aguirre, I.; Colín-Castro, C.A.; Morales-González, J.A.; Leyva-Gómez, G.; Magaña, J.J. Effect of UV and Gamma Irradiation Sterilization Processes in the Properties of Different Polymeric Nanoparticles for Biomedical Applications. *Materials* **2020**, *13*, 1090. https://doi.org/10.3390/ma13051090.
7. Raeiszadeh, M.; Adeli, B. A Critical Review on Ultraviolet Disinfection Systems against COVID-19 Outbreak: Applicability, Validation, and Safety Considerations. *ACS Photonics* **2020**, *7*, 2941–2951. https://doi.org/10.1021/acsphotonics.0c01245.
8. Igartua, M.; Hernández, R.M.; Rosas, J.E.; Patarroyo, M.E.; Pedraz, J.L. γ-Irradiation effects on biopharmaceutical properties of PLGA microspheres loaded with SPf66 synthetic vaccine. *Eur. J. Pharm. Biopharm.* **2008**, *69*, 519–526. https://doi.org/10/cr2vtz.
9. Domańska, I.M.; Oledzka, E.; Sobczak, M. Sterilization process of polyester based anticancer-drug delivery systems. *Int. J. Pharm.* **2020**, *587*, 119663. https://doi.org/10.1016/j.ijpharm.2020.119663.
10. Maksimenko, O.; Pavlov, E.; Toushov, E.; Molin, A.; Stukalov, Y.; Prudskova, T.; Feldman, V.; Kreuter, J.; Gelperina, S. Radiation sterilisation of doxorubicin bound to poly(butyl cyanoacrylate) nanoparticles. *Int. J. Pharm.* **2008**, *356*, 325–332. https://doi.org/10/bkcr7f.
11. Dorati, R.; Genta, I.; Montanari, L.; Cilurzo, F.; Buttafava, A.; Faucitano, A.; Conti, B. The effect of γ-irradiation on PLGA/PEG microspheres containing ovalbumin. *J. Control. Release* **2005**, *107*, 78–90. https://doi.org/10.1016/j.jconrel.2005.05.029.
12. Fernandezcarballido, A.; Puebla, P.; Herrerovanrell, R.; Pastoriza, P. Radiosterilisation of indomethacin PLGA/PEG-derivative microspheres: Protective effects of low temperature during gamma-irradiation. *Int. J. Pharm.* **2006**, *313*, 129–135. https://doi.org/10.1016/j.ijpharm.2006.01.034.
13. EMA. Guideline on the Sterilisation of the Medicinal Product, Active Substance, Excipient and Primary Container. EMA/CHMP/CVMP/QWP/850374/2015, European Medicines Agency, 2019. Available online: https://www.ema.europa.eu/en/documents/scientific-guideline/guideline-sterilisation-medicinal-product-active-substance-excipient-primary-container_en.pdf (accessed on 18 May 2023).
14. Sakar, F.; Özer, A.Y.; Erdogan, S.; Ekizoglu, M.; Kart, D.; Özalp, M.; Colak, S.; Zencir, Y. Nano drug delivery systems and gamma radiation sterilization. *Pharm. Dev. Technol.* **2017**, *22*, 775–784. https://doi.org/10/gfsj3j.
15. Athanasiou, K. Sterilization, toxicity, biocompatibility and clinical applications of polylactic acid/polyglycolic acid copolymers. *Biomaterials* **1996**, *17*, 93–102. https://doi.org/10/d95272.
16. Wang, J.; Ng, C.W.; Win, K.Y.; Shoemakers, P.; Lee, T.K.Y.; Feng, S.S.; Wang, C.H. Release of paclitaxel from polylactide-co-glycolide (PLGA) microparticles and discs under irradiation. *J. Microencapsul.* **2003**, *20*, 317–327. https://doi.org/10.3109/02652040309178072.

17. Song, T.-T.; Yuan, X.-B.; Sun, A.-P.; Wang, H.; Kang, C.-S.; Ren, Y.; He, B.; Sheng, J.; Pu, P.-Y. Preparation of injectable paclitaxel sustained release microspheres by spray drying for inhibition of glioma *in vitro*. *J. Appl. Polym. Sci.* **2010**, *115*, 1534–1539. https://doi.org/10.1002/app.31105.
18. Dobrzynski, P.; Kasperczyk, J.; Janeczek, H.; Bero, M. Synthesis of Biodegradable Copolymers with the Use of Low Toxic Zirconium Compounds. 1. Copolymerization of Glycolide with L -Lactide Initiated by $Zr(Acac)_4$. *Macromolecules* **2001**, *34*, 5090–5098. https://doi.org/10.1021/ma0018143.
19. Jing, Y.; Yang, M.; Dai, S.; Quan, C.; Liu, J.; Jiang, Q.; Zhang, C.; Liu, B. Microwaves promote transesterification in the rapid synthesis of methoxy-poly(ethylene glycol)-block-poly(l-lactide-random-glycolide). *Polymer* **2018**, *136*, 187–193. https://doi.org/10.1016/j.polymer.2017.12.062.
20. *EN ISO 10993-5:2009*; Biological Evaluation of Medical Devices—Part 5: Tests for In Vitro Cytotoxicity (ISO 10993-5:2009). Annex A Neutral Red Uptake (NRU) Cytotoxicity Test. International Organization for Standardization: Geneva, Switzerland, 2009.
21. *ISO/FDIS 13829:2000*. Water Quality-Determination of the Genotoxocity of Water and Waste Water Using the Umu-Test; International Organization for Standarization: Geneva, Switzerland, 2000.
22. Sarasua, J.-R.; Prud'homme, R.E.; Wisniewski, M.; Le Borgne, A.; Spassky, N. Crystallization and Melting Behavior of Polylactides. *Macromolecules* **1998**, *31*, 3895–3905. https://doi.org/10.1021/ma971545p.
23. Magazzini, L.; Grilli, S.; Fenni, S.E.; Donetti, A.; Cavallo, D.; Monticelli, O. The Blending of Poly(glycolic acid) with Polycaprolactone and Poly(l-lactide): Promising Combinations. *Polymers* **2021**, *13*, 2780. https://doi.org/10.3390/polym13162780.
24. Kasiński, A.; Zielińska-Pisklak, M.; Kowalczyk, S.; Plichta, A.; Zgadzaj, A.; Oledzka, E.; Sobczak, M. Synthesis and Characterization of New Biodegradable Injectable Thermosensitive Smart Hydrogels for 5-Fluorouracil Delivery. *Int. J. Mol. Sci.* **2021**, *22*, 8330. https://doi.org/10.3390/ijms22158330.
25. Dash, S.; Murthy, P.N.; Nath, L.; Chowdhury, P. Kinetic Modeling on Drug Release from Controlled Drug Delivery Systems. *Acta Pol. Pharm. Ñ Drug Res.* **2010**, *67*, 217–223.
26. Domańska, I.; Zalewska, A.; Cieśla, K.; Plichta, A.; Głuszewski, W.; Łyczko, M.; Kowalczyk, S.; Oledzka, E.; Sobczak, M. The influence of electron beam and gamma irradiation on paclitaxel-loaded nanoparticles of fully randomized copolymers in relation to potential sterilization. 2023, *manuscript submitted*.
27. Plikk, P.; Odelius, K.; Hakkarainen, M.; Albertsson, A.C. Finalizing the properties of porous scaffolds of aliphatic polyesters through radiation sterilization. *Biomaterials* **2006**, *27*, 5335–5347. https://doi.org/10/dwqz5s.
28. Loo, S.C.J.; Ooi, C.P.; Boey, Y.C.F. Radiation effects on poly(lactide-co-glycolide) (PLGA) and poly(l-lactide) (PLLA). *Polym. Degrad. Stab.* **2004**, *83*, 259–265. https://doi.org/10/c4fc7c.
29. Davison, L.; Themistou, E.; Buchanan, F.; Cunningham, E. Low temperature gamma sterilization of a bioresorbable polymer, PLGA. *Radiat. Phys. Chem.* **2018**, *143*, 27–32. https://doi.org/10.1016/j.radphyschem.2017.09.009.
30. Loo, J.S.C.; Ooi, C.P.; Boey, F.Y.C. Degradation of poly(lactide-co-glycolide) (PLGA) and poly(l-lactide) (PLLA) by electron beam radiation. *Biomaterials* **2005**, *26*, 1359–1367. https://doi.org/10/b2b29p.
31. Dorati, R.; Colonna, C.; Tomasi, C.; Bruni, G.; Genta, I.; Modena, T.; Conti, B. Long-Term Effect of Gamma Irradiation on the Functional Properties and Cytocompatibility of Multiblock Co-Polymer Films. *J. Biomater. Sci. Polym. Ed.* **2012**, *23*, 2223–2240. https://doi.org/10.1163/156856211X613915.
32. Walo, M.; Rzepna, M. *Recent Developments in Radiation Processing of Polymers*; Institute of Nuclear Chemistry and Technology: Warszawa, Poland, 2020.
33. Pandita, D.; Ahuja, A.; Velpandian, T.; Lather, V.; Dutta, T.; Khar, R.K. Characterization and in vitro assessment of paclitaxel loaded lipid nanoparticles formulated using modified solvent injection technique. *Pharmazie* **2009**, *64*, 301–310. https://doi.org/10.1691/ph.2009.8338.
34. Nandhakumar, S.; Dhanaraju, M.D.; Sundar, V.D.; Heera, B. Influence of surface charge on the in vitro protein adsorption and cell cytotoxicity of paclitaxel loaded poly(ε-caprolactone) nanoparticles. *Bull. Fac. Pharm. Cairo Univ.* **2017**, *55*, 249–258. https://doi.org/10.1016/j.bfopcu.2017.06.003.
35. Musumeci, T.; Ventura, C.; Giannone, I.; Ruozi, B.; Montenegro, L.; Pignatello, R.; Puglisi, G. PLA/PLGA nanoparticles for sustained release of docetaxel. *Int. J. Pharm.* **2006**, *325*, 172–179. https://doi.org/10.1016/j.ijpharm.2006.06.023.
36. Jusu, S.M.; Obayemi, J.D.; Salifu, A.A.; Nwazojie, C.C.; Uzonwanne, V.; Odusanya, O.S.; Soboyejo, W.O. Drug encapsulated blend of PLGA PEG microspheres: In vitro and in vivo study of the efects of localized/targeted drug delivery on the treatment of triple negative breast cancer. *Sci. Rep.* **2020**, *10*, 14188. https://doi.org/10.1038/s41598-020-71129-0.
37. Singhvi, G.; Singh, M. Review: In-Vitro Drug Release Characterization Models. *Int. J. Pharm. Stud. Res.* **2011**, *2*, 77–84.
38. Głuszewski, W.; Zagórski, Z.P. Radiation effects in polypropylene/polystyrene blends as the model of aromatic protection effects. *Nukleonika* **2008**, *53*, S21–S24.
39. Ferry, M.; Ngono, Y. Energy transfer in polymers submitted to ionizing radiation: A review. *Radiat. Phys. Chem.* **2021**, *180*, 109320. https://doi.org/10.1016/j.radphyschem.2020.109320.